# p53 functions as a negative regulator of osteoblastogenesis, osteoblast-dependent osteoclastogenesis, and bone remodeling

Xueying Wang,[1] Hui-Yi Kua,[1] Yuanyu Hu,[1] Ke Guo,[1] Qi Zeng,[1] Qiang Wu,[2] Huck-Hui Ng,[2] Gerard Karsenty,[3] Benoit de Crombrugghe,[4] James Yeh,[5] and Baojie Li[1]

[1]The Institute of Molecular and Cell Biology, Singapore 138673
[2]Laboratory of Cell and Medical Biology, Genome Institute of Singapore, Singapore 138672
[3]Department of Molecular and Human Genetics and Bone Disease Program of Texas, Baylor College of Medicine, Houston, TX 77030
[4]Department of Molecular Genetics, University of Texas M.D. Anderson Cancer Center, Houston, TX 77030
[5]Department of Medicine, Winthrop-University Hospital, Mineola, NY 11501

p53 is a well known tumor suppressor. We show that p53 also regulates osteoblast differentiation, bone formation, and osteoblast-dependent osteoclast differentiation. Indeed, $p53^{-/-}$ mice display a high bone mass phenotype, and $p53^{-/-}$ osteoblasts show accelerated differentiation, secondary to an increase in expression of the osteoblast differentiation factor osterix, as a result. Reporter assays indicate that p53 represses osterix transcription by the minimal promoter in a DNA-binding–independent manner. In addition, $p53^{-/-}$ osteoblasts have an enhanced ability to favor osteoclast differentiation, in association with an increase in expression of macrophage-colony stimulating factor, which is under the control of osterix. Furthermore, inactivating p53 is sufficient to rescue the osteoblast differentiation defects observed in mice lacking c-Abl, a p53-interacting protein. Thus, these results identify p53 as a novel regulator of osteoblast differentiation, osteoblast-dependent osteoclastogenesis, and bone remodeling.

## Introduction

The major role of p53 is to promote cell cycle arrest, programmed cell death, and cell senescence, and it is mutated in more than half of the primary human tumors (Ko and Prives, 1996; Vogelstein et al., 2000). p53 executes its function mainly by activating the transcription of target genes involved in these cellular events, in which the binding of p53 to a specific DNA sequence is necessary (Giaccia and Kastan, 1998; Oren, 1999). p53 can also act as a transcription repressor (Yu et al., 1999). In some cases, the repression is independent of DNA binding (Agoff et al., 1993; Zhai and Comai, 2000; Crighton et al., 2003; Rocha et al., 2003). p53 can be brought to the promoter regions of these genes through other DNA-binding proteins, such as the CAAT-binding factor (Zhai and Comai, 2000), where p53 may interfere with the assembly of the transcription–initiation complex (Zhai and Comai, 2000) or recruit transcription repressors like histone deacetylase (Murphy et al., 1999; Rocha et al., 2003). Hence, p53 can repress gene expression using complex and diverse mechanisms, most of which are not well understood. In addition, the biological significance of p53-mediated repression remains unclear (Ho and Benchimol, 2003).

p53 has also been implicated in cell differentiation and mouse development, although initial studies of $p53^{-/-}$ mice did not reveal any developmental abnormalities (Donehower et al., 1992; Almog and Rotter, 1997; Choi and Donehower, 1999). It has been reported that a small portion of homozygous embryos displayed a neural tube closure defect called exencephaly and that $p53^{-/-}$ embryos were more susceptible to teratological reagents (Sah et al., 1995; Hall and Lane, 1997), yet, the molecular mechanisms through which p53 regulates cell differentiation and mouse development remain largely unknown.

We have previously established that the nonreceptor tyrosine kinase c-Abl plays a positive role in murine osteoblast differentiation and bone development (Li et al., 2000). Given the functional relationship between c-Abl and p53, we decided to study the role of p53 in osteoblast differentiation and bone remodeling. Osteoblast is a cell of mesenchymal origin that is responsible for bone formation and can support osteoclast

Correspondence to Baojie Li: libj@imcb.a-star.edu.sg

Abbreviations used in this paper: ALP, alkaline phosphatase; BMM, bone marrow monocyte; BMP, bone morphogenetic protein; cDNA, complementary DNA; M-CSF, macrophage-colony stimulating factor; MEF, mouse embryonic fibroblast; OPG, osteoprotegerin; RANKL, receptor activator of NFκB ligand; siRNA, small interfering RNA; TBP, thyroxine-binding protein; TRAP, tartrate-resistant acid phosphatase.


The Journal of Cell Biology, Vol. 172, No. 1, January 2, 2006 115–125
http://www.jcb.org/cgi/doi/10.1083/jcb.200507106

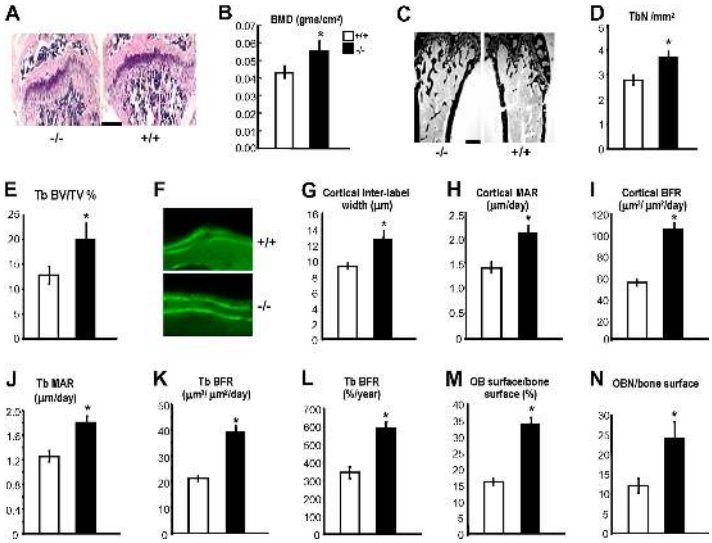


Figure 1. **Mice deficient for p53 showed increased bone mass and increased bone formation rates.** (A) Normal growth plates in $p53^{-/-}$ mice. Femurs were fixed, decalcified, and stained with hematoxylin-eosin. (B) Bone mineral density (BMD) of the mutant and wild-type mice of the same age and gender. Femur bones were taken from 3–4-mo-old p53 knockout and control mice and their bone densities measured ($n = 8$, $P = 0.004$). (C) A representative von Kossa staining of the femurs of mutant and control mice showing an overall improved trabecular bone in $p53^{-/-}$ mice. (D) The number of trabecular bones was increased in $p53^{-/-}$ mice ($n = 8$, $P = 0.014$). (E) $p53^{-/-}$ mice had increased trabecular bones (trabecular bone vol/tissue vol; $n = 8$, $P = 0.0037$). (F) Calcein labeling of the cortical bones in mutant and control mice. 3–4-mo-old mice were injected with calcein twice, with an interval of 9 d. The mice were killed and femur bones sectioned without decalcification. Pictures were taken under a fluorescence microscope (40×). (G) Interlabel width (μm; $n = 8$, $P = 0.025$). (H) Mineral apposition rates ($n = 8$, $P = 0.025$). (I) Bone formation per bone perimeter. ($n = 8$, $P = 0.0004$) (J) Mineral apposition rates in trabecular bones ($n = 8$, $P = 0.03$). (K) Trabecular bone formation rates per bone perimeter ($n = 8$, $P = 0.032$). (L) Bone formation rate per bone area in trabecular bones ($n = 8$, $P = 0.032$). (M) $p53^{-/-}$ mice showed increased osteoblast surface (osteoblast surface/bone surface; $n = 5$, $P = 0.012$). (N) $p53^{-/-}$ mice showed increased osteoblast numbers (osteoblast numbers/bone surface; $n = 5$, $P = 0.034$). Bar, 500 μm. Error bars represent ± SD. Asterisks mark samples significantly different from control with $P < 0.05$.

differentiation. Over the last 10 yr, a growing body of knowledge has emerged regarding the transcriptional control of osteoblast differentiation and function. Runx2 is the earliest determinant of osteoblast differentiation, and its expression defines a bipotential cell type called an osteochondroprogenitor (Ducy et al., 1997). Downstream of Runx2, other osteoblast-specific transcription factors have been identified. One is osterix, which has mainly been studied in a developmental context until this point (Nakashima et al., 2002). The other is ATF4, which controls both osteoblast differentiation and function (Yang et al., 2004; Elefteriou et al., 2005). We report that p53 negatively regulates osteoblast differentiation and function by repressing the expression of osterix. The level of osterix, but not that of Runx2 or ATF4, was elevated in osteoblasts and the bones of $p53^{-/-}$ mice, and elevated expression of p53 inhibited osterix expression and the *Osx* promoter activity in a p53-binding–independent manner. Moreover, p53 deficiency conferred the osteoblasts with an increased ability to promote osteoclastogenesis, most likely through the up-regulation of macrophage-colony stimulating factor (M-CSF). This study adds to our current knowledge of osteoblast differentiation, osteoblast-supported osteoclastogenesis, bone remodeling, and the developmental role of the tumor suppressor p53.

## Results

### $p53^{-/-}$ mice showed increased bone mass and increased bone formation

To determine whether p53 has a role in the skeleton, we analyzed bones from 3–4-mo-old wild-type and $p53^{-/-}$ mice. No evident abnormality was observed in the gross development of the skeleton. Histological analysis of hematoxylin-eosin–stained long bone sections indicated that the growth plates were not significantly altered either (Fig. 1 A). However, dual x-ray absorptiometry analysis of eight $p53^{-/-}$ mice and their littermate controls revealed that $p53^{-/-}$ mice showed a modest but consistent increase in bone mineral density (Fig. 1 B). von Kossa staining and bone histomorphometric analysis of the sectioned long bones revealed that $p53^{-/-}$ mice had a 29% increase in the number of trabecular bones and a 40% increase in the volume of trabecular bones (Fig. 1, C–E). A slight increase was detected in the volume of cortical bones (45.7 ± 2.8% [bone vol/tissue vol] for +/+ vs. 52.4 ± 2.7% for −/− of femurs, $n = 8$, $P = 0.035$). In vivo calcein labeling revealed that $p53^{-/-}$ mice consistently showed a marked increase in the mineral apposition rate and bone formation rates at the periosteal surface (Fig. 1, F–I), as well as in the trabecular bones (Fig. 1, J–L), but not at the endosteal surface (not depicted). Additionally, $p53^{-/-}$ mice also showed a marked increase in the osteoblast surface and the number of osteoblasts per bone surface (Fig. 1, M and N). Together, these results established that p53 exerts a negative influence on osteoblast differentiation and/or function.

### $p53^{-/-}$ osteoblasts showed increased proliferation rates and accelerated differentiation

In an effort to decipher the cellular mechanisms leading to the increase in bone mass observed in $p53^{-/-}$ mice, we first wanted to determine whether the bone marrow contains the same number of osteoprogenitor cells as in control mice. Total bone marrow cells were counted and directly plated in a 35-mm plate. The alkaline phosphatase (ALP) colony–forming units and total colony-forming units were comparable between $p53^{-/-}$ and control mice (Fig. 2 A), suggesting that p53 deficiency did not significantly alter the differentiation potential of mesenchymal cells into osteoblasts.

To attest that p53 negatively regulates osteoblast differentiation, we isolated calvarial primary osteoblasts from wild-type and $p53^{-/-}$ mice. Differentiation assays showed that $p53^{-/-}$ osteoblasts expressed more ALP (Fig. 2 B), with the p53 heterozygous culture displaying an intermediate phenotype.

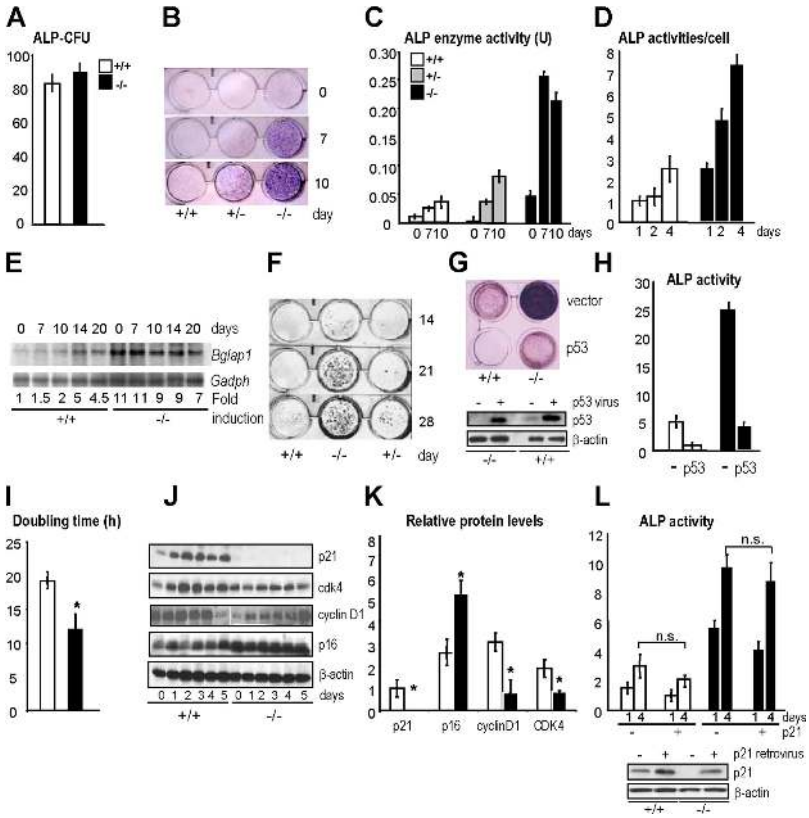


Figure 2. **Calvarial osteoblasts showed enhanced differentiation.** (A) p53 deficiency did not significantly alter the differentiation potential of mesenchymal cells into osteoblasts. Colonies containing >25 cells were counted (per $2.5 \times 10^6$ bone marrow cells). (B) Calvarial osteoblasts were isolated from newborn mice and cultured to passage 3. The same number of cells was then plated into 12-well plates at $2.5 \times 10^5$ per well. (C) Quantitation of ALP activities of $p53^{-/-}$ and control wild-type cells that were normalized to protein levels. (D) Quantitation of ALP activities of $p53^{-/-}$ and control wild-type cells that were normalized to the number of cells. The ALP activity for control cells at day 1 was set at 1. (E) Northern blot analysis shows that expression of osteocalcin during differentiation of $p53^{-/-}$ and control calvarial osteoblasts. The level of osteocalcin in control osteoblasts at day 0 was set at 1. (F) Osteoblasts were cultured as in B, except that the cells were stained using the von Kossa method for mineral deposition. (G and H) Reconstitution of p53 led to normal differentiation of $p53^{-/-}$ osteoblasts, justified by ALP staining (G) and quantitative ALP (H). (G, bottom) Expression of p53 in mutant and control cells. (I) $p53^{-/-}$osteoblasts showed reduced doubling time. $4 \times 10^5$ cells (triplicates) were plated in 60-mm plates, and the number of cells were counted every day for 5 d and plotted. Doubling time was calculated from three $p53^{-/-}$ osteoblasts and their control littermates. (J) Expression of proteins involved in cell proliferation. The experiments were carried out as described in I, and one plate was harvested each day for Western blot analysis. (K) Quantitation data (day 3) for the data presented in J. (L) Retroviral expression of p21 in $p53^{-/-}$ osteoblasts did not significantly repress differentiation. $p53^{-/-}$ and control osteoblasts were infected with p21-expressing retrovirus (or control retrovirus), selected for 5 d, and plated for ALP assays. Error bars represent ± SD. Asterisks mark samples significantly different from control with $P < 0.05$.

Quantitative assays for ALP (enzyme activities normalized to total protein levels or the number of osteoblasts) confirmed the results obtained from histological staining (Fig. 2, C and D). During the second to third week in culture, osteoblasts start to express osteocalcin (*Bglap1*), an osteoblast-specific gene that is a marker of fully differentiated osteoblasts and is involved in osteogenesis. Wild-type osteoblasts exhibited a gradual increase in osteocalcin levels over time, whereas $p53^{-/-}$ osteoblasts expressed maximal osteocalcin from day 0 of culture, suggesting that p53 negatively regulates osteocalcin expression (Fig. 2 E). Similarly, increased nodule formation or bone mineralization was observed in p53 null osteoblast cultures (Fig. 2 F), and reconstitution of p53 by retroviral infection blocked the accelerated differentiation of $p53^{-/-}$ osteoblasts and retroviral expression of p53 in control cells inhibited their differentiation (Fig. 2, G and H). Enhanced osteoblast differentiation was also observed in bone marrow stromal cultures of $p53^{-/-}$ mice (unpublished data). These results indicate that the biological function of p53 in cells of the osteoblast lineage is to inhibit or slow down their differentiation.

To test whether p53 affects proliferation of osteoblasts, we compared the growth rates of $p53^{-/-}$ and control osteoblasts and found that in the absence of p53 osteoblasts doubled at a higher rate (Fig. 2 I). This may explain why $p53^{-/-}$ mice exhibit an increased number of osteoblasts in vivo. Western blot analysis revealed that expression of the cyclin-dependent kinase inhibitor p21was abolished in $p53^{-/-}$ cells (Fig. 2, J and K). This may explain why p53 osteoblasts have a shorter cell cycle. Surprisingly, we found that in $p53^{-/-}$ cells the levels of $p16^{ink4}$ were up-regulated, whereas cyclin-dependent kinase 4 and cyclin D1 were down-regulated (Fig. 2 , J and K). This may reflect a compensation mechanism for the loss of p53. To confirm that enhanced differentiation is not caused by accelerated proliferation, we expressed p21 in $p53^{-/-}$ osteoblasts with a retrovirus and found that cell proliferation rates were down to those of control osteoblasts (not depicted), yet these osteoblasts still exhibited enhanced differentiation (Fig. 2 L), suggesting that enhanced differentiation caused by p53 deficiency is independent of cell proliferation.

## Up-regulation of osterix in $p53^{-/-}$ osteoblasts and mice

To determine the molecular basis of p53 action in osteoblast, we next asked whether it could influence expression or function of the known osteoblast-specific transcription factors such as Runx2, Osterix, and ATF4. Total RNA was isolated from $p53^{-/-}$ and control osteoblasts at different stages of differentiation and used for RT-PCR assays. No dramatic up-regulation of Runx2 was observed during differentiation of mutant or control cells. Nor was there a significant difference in the basal levels of Runx2 or ATF4 between $p53^{-/-}$ and control osteoblasts (Fig. 3, A and C; and not depicted). On the other hand, $p53^{-/-}$ osteoblasts showed a significant elevation of osterix at the basal level (Fig. 3 A). In both $p53^{-/-}$ and control osteoblasts,

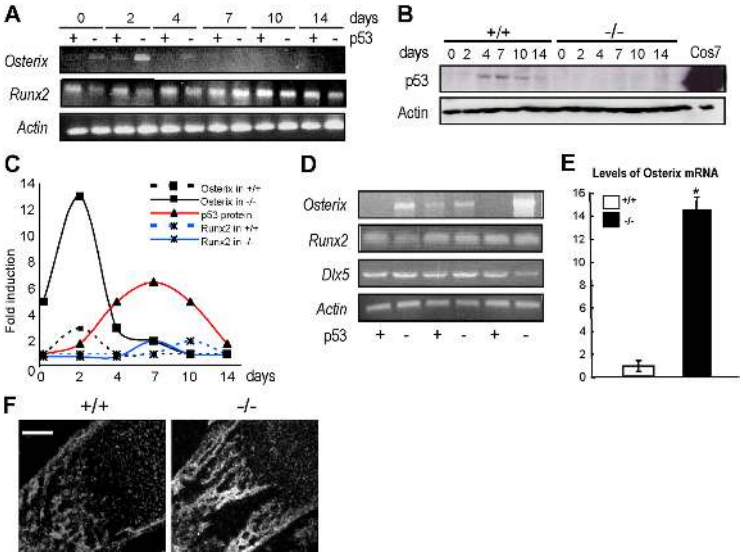


Figure 3. **Osteoblasts deficient for p53 showed up-regulated expression of osterix, but not Runx2.** (A) Mutant and control osteoblasts were collected at different stages of differentiation. Total RNA was isolated and used for RT-PCR. (B) Expression of p53 changed during osteoblast differentiation. Cells at different stages of differentiation were harvested and the levels of p53 were determined by Western blot analysis. (C) Quantitation data from A and B (similar results were obtained from four pairs of $p53^{-/-}$ and control osteoblasts). The level of osterix, Runx2, or p53 in control osteoblast was set at 1. (D and E) Elevated expression of osterix mRNA in calvaria of $p53^{-/-}$ mice. Total RNA was made from calvaria of $p53^{-/-}$ and control mice and used for RT-PCR for osterix, Runx2, and Dlx5 (D), or real-time PCR for osterix (E) to assess the mRNA levels of osterix. The level of osterix mRNA in control calvaria was set at 1. The internal control for real-time PCR was GADPH mRNA. (F) In situ staining of osterix mRNA. Femurs of $p53^{-/-}$ and control mice were OCT embedded and cryosectioned, fixed, and then hybridized with radio-labeled osterix antisense RNA probe. Osterix is mainly expressed at sites of mature osteoblasts beneath the growth plates. Bar, 500 μm. Error bars represent ± SD. Asterisks mark samples significantly different from control with $P < 0.05$.

expression of osterix peaked rapidly at day 2 and subsided to basal levels later on. Still, $p53^{-/-}$ osteoblasts displayed a much higher peak value than control cells. This up-regulation of osterix could be a cell response to bone morphogenetic proteins (BMPs) that are secreted by osteoblasts. The results suggest that the effect of p53 on osteoblast differentiation is downstream of Runx2 and upstream of osterix. Note that p53 levels started to increase at day 4 during differentiation, and the significance of this regulation warrants further investigation (Fig. 3 B). Moreover, we found that osterix, but not other transcription factors, was up-regulated in calvarial bones of $p53^{-/-}$ mice (Fig. 3, D and E). In situ hybridization using RNA probes generated from the osterix coding sequence confirmed the results (Fig. 3 F and not depicted). Overall, these results suggest that one function of p53 is to inhibit osterix expression and, hence, osteoblast differentiation.

## p53 repressed the promoter activity of osterix

Two experiments further support that p53 plays a negative role in osterix expression. Primary mouse embryonic fibroblasts (MEFs), when stimulated with BMP2, start to express osteoblast-specific markers. We found that osterix was markedly induced in $p53^{-/-}$ MEFs compared with control cells, in response to a short-term treatment with BMP2 (Fig. 4 A). Furthermore, when p53 was up-regulated by the DNA damage reagent cisplatin it repressed the expression of osterix in wild-type primary osteoblasts, but not in $p53^{-/-}$ osteoblasts (Fig. 4 B). These results confirmed that p53 is a negative regulator of osterix.

To test whether p53 represses the transcription of osterix, a 6.0-kb DNA fragment upstream of the transcription start site of osterix gene (*Osx*) was fused to the luciferase gene in pGL3 basic vector. Coexpression of p53 led to a dosage-dependent repression of *Osx* promoter activity in C2C12 and MC3T3-E1 cells (Fig. 4 C and not depicted). p53R273H, a mutant with no DNA-binding ability, still significantly repressed *Osx* promoter (Fig. 4 D), suggesting that DNA binding may not be required. Moreover, p53S15A, a mutation of a phosphorylation site important for transactivation of p53 target genes in response to DNA damage, could repress the *Osx* promoter. On the other hand, p53 mutants such as p53Δ62-91 (the proline-rich domain deleted), p53M246I (point mutation in the DNA-binding domain), and p53L22Q/W23S (two point mutations that abolish p53 transactivation activity), which were reported to have dramatically reduced the ability to repress other p53 target genes (Murphy et al., 1996; Venot et al., 1998; Roth et al., 2000), failed to repress the *Osx* promoter (Fig. 4 D). These results suggest that p53 might repress *Osx* promoter activity with a common mechanism.

The following observations suggest that p53 represses the *Osx* promoter independent of DNA binding. First, no canonical p53-binding site was present in the 6-kb promoter sequence. Second, serial deletion experiments indicated that all fragments (6, 4, 2, 1.0, 0.5, 0.3, and 0.13 kb upstream of the start site) could still be repressed by p53 (Fig. 4 E). This 0.13-kb fragment contains mainly the TATA box–like sequence and is a minimal sequence that retains some activity in a reporter assay. Third, chromatin immunoprecipitation assays demonstrated that p53 was not directly associated with the 2-kb sequence of the osterix promoter even though its binding was detectable at the p21 promoter (unpublished data). These results suggest that p53 repressed osterix transcription independent of its binding to the upstream activation sequence.

We also found that p300, among several transcription factors and coactivators, could activate the *Osx* promoter, and that this activation was repressed by p53 as well (Fig. 4 F). Because p300 is expressed in the cells at a limiting concentration, it is possible that p53 subjugates this coactivator to repress gene transcription, as proposed previously (Vo and Goodman, 2001; Soussi and Lozano, 2005). To date, p53 has been reported to inhibit the transcription of many genes like *Osx*. Yet, the molecular mechanisms behind the repression are not well understood. This prevents us from establishing the exact role of p53 in the repression of *Osx* transcription.

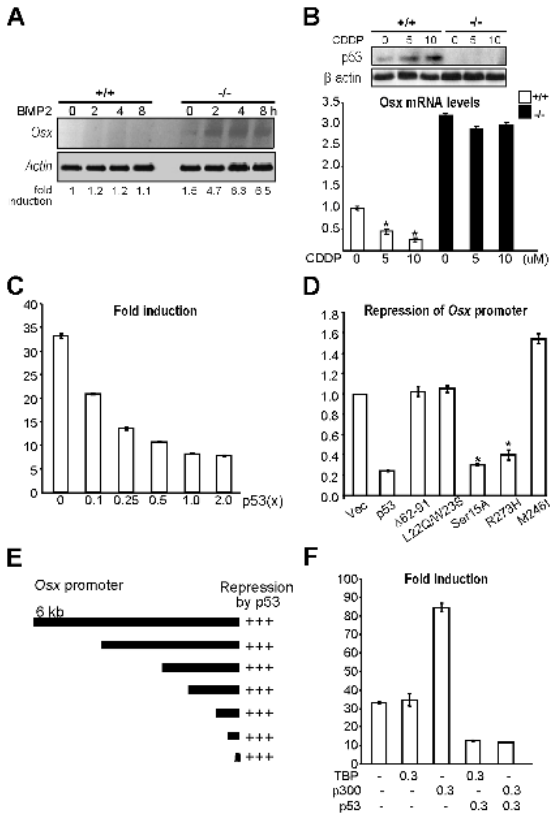


Figure 4. **p53 inhibited the promoter activity of osterix.** (A) Induction of osterix mRNA by BMP2 in $p53^{-/-}$ and control MEFs. MEFs were stimulated with 100 ng/ml BMP2 for different periods of time. Total RNA was isolated, and RT-PCR was performed. Similar results were obtained from three pairs of mutant and control MEFs. The level of osterix in control cells at time 0 was set at 1. (B) DNA damage inhibited the expression of osterix. $p53^{-/-}$ and control osteoblasts were treated with 5 or 10 μM of cisplatin for 24 h, and total RNA was isolated for RT-PCR assays. (bottom) The values of the Y axis were normalized to the level of actin, with the basal level of control cells set at 1. (top) Western blot analysis of p53 induction by cisplatin in control osteoblasts. *, $P < 0.05$, compared with the same genotype without CDDP treatment. (C) Coexpression of p53 inhibited the basal level of the promoter activity in osterix promoter-Luc. (D) Effects of p53 mutants on osterix promoter activity. Each of these p53 mutant constructs was cotransfected into C2C12 cells with the reporter gene, and luciferase activity was measured. (E) Serial deletion analysis of the osterix promoter. Different constructs were cotransfected into C2C12 cells with 1× p53 expression construct and the luciferase activities were measured as in C. The repression was compared with the 6-kb promoter (+++). (F) p53 repressed *Osx* promoter activity in the presence of p300. The experiments were performed as in D, except that TBP or p300 was included. 0.3 μg DNA was used for each expression construct. Error bars represent ± SD.

## Elevated osterix mediated the enhanced differentiation of $p53^{-/-}$ osteoblasts

We then attempted to determine whether elevation in osterix mediated the enhanced differentiation of $p53^{-/-}$ osteoblasts. We first tested whether osterix overexpression could lead to enhanced differentiation. $p53^{-/-}$ and control osteoblasts were infected with retroviruses expressing osterix, selected against puromycin for 3 d, and then used for ALP or osteocalcin assays (Fig. 5, A–E). We observed a retroviral dose-dependent increase in osterix levels (Fig. 5, B and D), which was likely caused by multiple infections in a single cell. An up-regulation in ALP activities and osteocalcin was also seen (Fig. 5, A, C, and E). When retrovirus-infected wild-type osteoblasts expressed osterix to the level of $p53^{-/-}$ osteoblasts, they expressed similar levels of ALP and osteocalcin as $p53^{-/-}$ cells (Fig. 5, C and E). These results indicate that elevation of osterix could promote osteoblast differentiation and the enhanced differentiation of $p53^{-/-}$ osteoblasts might be at least partially mediated by the increased expression of osterix. Second, we attempted to determine whether increased osterix expression was required for the enhanced differentiation of $p53^{-/-}$ osteoblasts. Small interfering RNA (siRNA)–mediated knocking down of osterix was performed in control and $p53^{-/-}$ osteoblasts and osteoblast differentiation markers were analyzed (Fig. 5, F–J). Different combinations of siRNA species reduced osterix to different levels (Fig. 5, G and I), leading to decreased expression of ALP and osteocalcin (Fig. 5, F–H and J). The results suggested that osterix was necessary for osteoblast differentiation and that the effect of p53 on osteoblast differentiation might be at least partially mediated by osterix.

## $p53^{-/-}$ osteoclasts showed normal differentiation and resorption in culture

Increased bone mass could be attributed to reduced bone resorption, in addition to increased bone formation. Further analysis revealed an unanticipated result. $p53^{-/-}$ mice showed a onefold increase in the bone resorption surface and the number of osteoclasts (Fig. 6, A and B). $p53^{-/-}$ mice also showed an increase in the excretion of urine deoxypyridinoline cross-links (Fig. 6 C). These data indicate that $p53^{-/-}$ mice have increased bone resorption in addition to increased bone formation. This may explain why $p53^{-/-}$ mice only showed modest osteosclerotic phenotypes despite bone formation rates being nearly double that of control mice.

To determine whether deficiency of p53 has a cell-autonomous effect on osteoclasts, we analyzed osteoclastogenesis and osteoclast resorption of $p53^{-/-}$ and control bone marrow monocytes (BMMs) in the presence of M-CSF and receptor activator of NFκB ligand (RANKL), which are necessary and sufficient for osteoclast proliferation and differentiation. No significant difference was observed in the number of osteoclasts formed from $p53^{-/-}$ and control BMMs (Fig. 6, D and E) nor did we observe a significant difference in the bone resorption activities of the $p53^{-/-}$ and control osteoclast cultures based on pit formation on dentine slices (Fig. 6, F and G). These results suggest that p53 has no cell-autonomous effect on the differentiation and the function of osteoclasts.

## $p53^{-/-}$ osteoblasts had increased osteoclastogenic capabilities secondary to an increase in M-CSF

The aforementioned findings raised the possibility that increased activities of $p53^{-/-}$ osteoblasts led to increased osteoclastogenesis and bone resorption in vivo. It has been well established that osteoblasts control osteoclast differentiation by synthesizing M-CSF, RANKL, and osteoprotegerin (OPG, a RANKL decoy receptor; Suda et al., 1999; Boyle et al., 2003). To prove this, we cocultured primary calvarial osteoblasts ($p53^{-/-}$ or control)

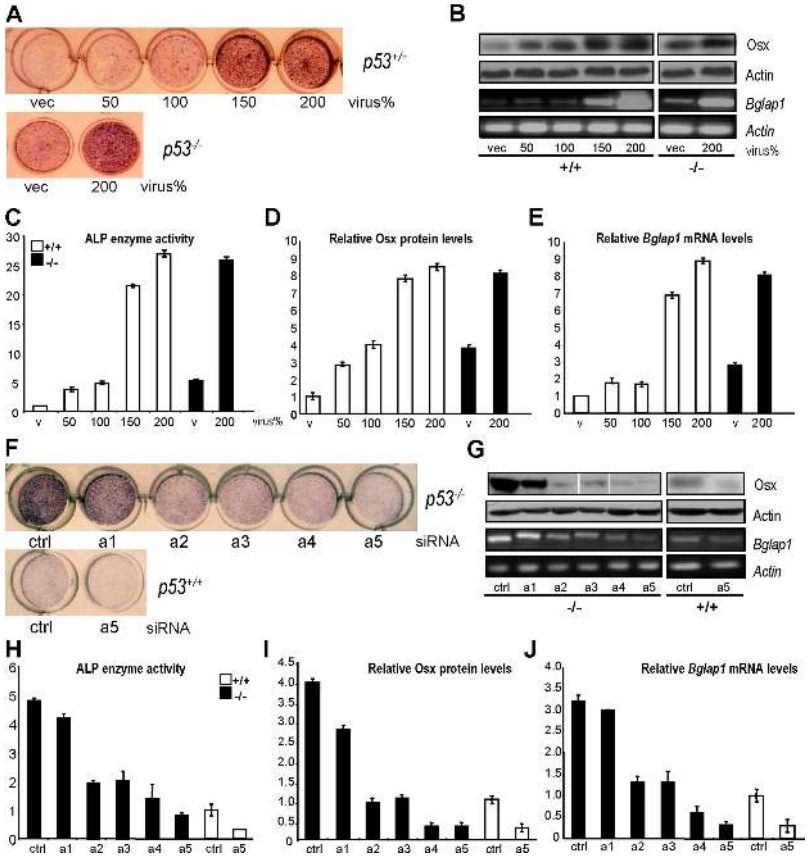


Figure 5. **Elevated expression of osterix was necessary and sufficient for accelerated differentiation of $p53^{-/-}$ osteoblasts.** (A) Ectopic expression of osterix led to increased expression of the osteoblast marker ALP. Wild-type primary osteoblasts were infected with increasing amounts of retrovirus expressing osterix, selected for 3 d, and stained for ALP. (B) Western blot analysis showed the levels of osterix in cells infected with the retrovirus (top). RT-PCR assays showed the increase of osteoblast marker osteocalcin in response to ectopic expression of osterix (bottom). (C) ALP activities normalized to the level of proteins. Control cells infected with vector were set at 1. (D) Quantitation data for the protein levels of osterix in B. Control cells infected with vector were set at 1. (E) Quantitation data for the mRNA levels of osteocalcin in B. Control cells infected with vector were set at 1. (F) Knocking down of osterix (a1 to a5) led to a reduction in ALP expression in $p53^{-/-}$ osteoblasts. $p53^{-/-}$ and control osteoblasts were transfected with siRNA against osterix and control oligos for 2 d and the plates were stained for ALP. Different combinations of four commercially designed siRNA species were used to obtain different degrees of knocking down. a1, 1+2 siRNA duplexes; a2, 3+4 duplexes; a3, 1–4 duplexes; a4, 1–4 duplexes (2×); a5, 1–4 duplexes (4×). (G) Western blot analysis showed the levels of osterix in cells transfected with siRNAs (top). RT-PCR assays showed the decrease of osteoblast marker osteocalcin in response to knocking down of osterix (bottom). (H) ALP activities normalized to the level of proteins. Control cells transfected with control siRNAs was set at 1. (I) Quantitation data for the protein levels of osterix in H. Control cells transfected with control siRNAs were set at 1. (J) Quantitation data for the mRNA levels of osteocalcin in H. Control cells transfected with control siRNAs were set at 1. Error bars represent ± SD.

with BMMs ($p53^{-/-}$ or control) in the presence of $10^{-8}$ M dihydroxyvitamin D3, and stained for tartrate-resistant acid phosphatase (TRAP)–positive cells (Fig. 6, H and I). Primary osteoblasts were plated at a high density so that the plates would become confluent overnight. This was to eliminate any possible effects of growth disparity of osteoblasts. These TRAP-positive osteoclasts were much smaller, compared with those formed in the presence of M-CSF and RANKL (Fig. 6 D), with a small multinucleated portion, similar to what has been observed in previous studies (Geoffroy et al., 2002). Nevertheless, $p53^{-/-}$ osteoblasts exhibited a marked increase in the number of TRAP-positive osteoclasts regardless of the genotype of BMMs, compared with $p53^{+/+}$ osteoblasts. When only cells with ≥3 nuclei were counted, a 2.5-fold increase was observed for monocytes (both $p53^{+/+}$ and $p53^{-/-}$) cultured on $p53^{-/-}$ osteoblasts, compared with those cultured on control osteoblasts (Fig. 6 J). $p53^{-/-}$ and $p53^{+/+}$ monocytes behaved similarly when cultured on $p53^{-/-}$ osteoblasts or wild-type osteoblasts, confirming that p53 did not have a cell-autonomous effect on osteoclastogenesis (Fig. 6, D and E). These results indicated that osteoblasts deficient for p53 had increased potentials in promoting osteoclastogenesis and that the increased osteoclast number and bone resorption observed in $p53^{-/-}$ mice might be attributable to the enhanced activities of $p53^{-/-}$ osteoblasts. In accordance with the enhanced osteoclastogenesis, RT-PCR analysis revealed a significant increase in the level of M-CSF in $p53^{-/-}$ osteoblasts, but not of RANKL or OPG (Fig. 6 K and not depicted). M-CSF controls both the proliferation and the differentiation of osteoclasts (Tanaka et al., 1993; Sarma and Flanagan, 1996). Moreover, ectopic expression of osterix in primary cells was found to increase the level of M-CSF in a dosage-dependent manner (Fig. 6 L), suggesting that the enhanced osteoclastogenesis capacity of $p53^{-/-}$ osteoblasts may be attributable to the elevated expression of osterix.

## p53 acted downstream of c-Abl in osteoblast differentiation

Mice deficient for c-Abl show signs of osteoporosis, and the mutant osteoblasts show defects in differentiation and survival against oxidative stress (Li et al., 2000, 2004). Because p53 is a c-Abl–interacting protein and genetically interacts with c-Abl during cell proliferation and apoptosis (Whang et al., 2000; Deng et al., 2004), we studied their relationship in bone development. Unfortunately, compound homozygous mice for c-Abl and p53 were very difficult to obtain, probably owing to the embryonic and/or postnatal lethality of these mice. Nevertheless, we isolated calvarial osteoblasts from four 20-d embryos of double homozygous mice and control littermates, and compared their differentiation potential. The compound knockout cells behaved similarly to $p53^{-/-}$ osteoblasts in ALP expression and in mineral deposition (Fig. 7, A–C). Real-time PCR assays indicated that osterix expression was down-regulated in c-Abl–deficient cells but up-regulated in the compound double knockout mice, resembling $p53^{-/-}$ osteoblasts (Fig. 7 D). These data suggest that p53 functions downstream of c-Abl in the process of osteoblast differentiation.

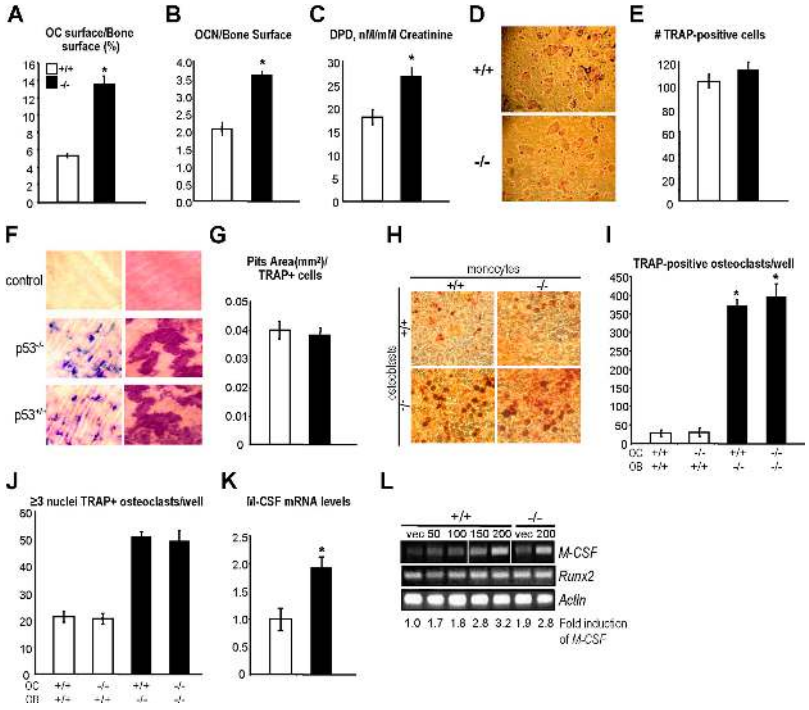


Figure 6. **Effects of p53 deficiency on osteoclast differentiation and resorption.** (A) $p53^{-/-}$ mice showed increased osteoclast surface (osteoclast surface/bone surface). $n = 8$, $P = 0.013$. (B) $p53^{-/-}$ mice showed an increase in the number of osteoclasts per bone surface. $n = 8$, $P = 0.002$. (C) Urinary deoxypyridinoline (DPD) cross-links excretion was significantly increased in *p53*-deficient mice compared with control mice. (D) Normal osteoclast differentiation from BMMs in $p53^{-/-}$ mice in the presence of M-CSF and RANKL. (E) Quantitation data from five $p53^{-/-}$ and control littermate mice. (F) Normal bone resorption rates of $p53^{-/-}$ osteoclasts. Pit formation assays of $p53^{-/-}$ and control osteoblasts (two representative views of different magnifications; left, stained with Toluidine blue; right, stained with Gill's Hematoxylin Solution). (G) Quantitation of the resorption area by $p53^{-/-}$ and control osteoblasts ($n = 4$). (H) $p53^{-/-}$ osteoblasts showed a much greater stimulatory effect on osteoclastogenesis. $p53^{-/-}$ and control osteoblasts were first plated, and then the BMMs isolated from $p53^{-/-}$ and control mice were plated. They were cocultured for 6 d in the presence of $10^{-8}$ M of vitamin D3 and stained for TRAP-positive osteoclasts. (I) Quantitation data from H ($n = 4$). (J) Number of TRAP-positive cells per well with ≥3 nuclei. *, $P < 0.05$, comparison between osteoclastogenesis (+/+ or −/− monocytes) on +/+ and −/− osteoblasts. (K) Up-regulation of M-CSF in $p53^{-/-}$ osteoblasts. PT-PCR analysis of the mRNA levels of M-CSF in $p53^{-/-}$ and control osteoblasts. The levels of M-CSF mRNA for control cells were set at 1. (L) Ectopic expression of osterix increased the expression of M-CSF. RT-PCR was performed for the sample used in Fig. 5 A. Error bars represent ± SD.

## Discussion

We provide genetic evidence that p53 plays a negative role in postnatal bone development, with a cell-autonomous effect on osteoblastogenesis. The mice deficient for p53 displayed increased bone formation and osteosclerotic phenotypes; the osteoblasts deficient for p53 showed enhanced proliferation and accelerated differentiation; and p53 deficiency could overcome the differentiation defects of $c\text{-}Abl^{-/-}$ osteoblasts. Moreover, p53 deficiency confers the osteoblasts a greater osteoclastogenic capacity, without directly affecting osteoclast differentiation or resorption. Accordingly, increased bone resorption was also observed in $p53^{-/-}$ mice. Thus, the osteosclerotic phenotype is a net result of the direct effect of p53 on osteoblast action combined with an osteoblast-mediated effect on osteoclasts. This osteoblast-supported osteoclastogenesis might explain why most of the osteosclerosis models associated with enhanced osteoblast function do not exhibit a huge increase in bone mass (Ducy et al., 1996, 2000; Manolagas and Jilka, 1995; Sabatakos et al., 2000).

The conclusion that p53 plays a negative role in osteoblastogenesis is supported by the findings that p53 might directly regulate the expression of osteocalcin (Schwartz et al., 1999; Chandar et al., 2000). However, our results are not in agreement with a recent study stating that p53 did not affect osteoblast differentiation and mouse bone formation, although they did show that p53 deficiency rescued the bone loss induced by mechanical unloading (Sakai et al., 2002). The discrepancy could be caused by the genetic background (C57BL/6 in our studies, but not mentioned by Sakai et al., 2002) or the age of the mice used (4 mo in our studies vs. 2 mo in the Sakai study), and warrants further investigation. Nevertheless, our results obtained from studies on whole mice, the bones, the cells involved, and the participating molecules convincingly support a negative role for p53 in osteoblastogenesis and bone formation that contributes to the osteosclerotic phenotype observed in $p53^{-/-}$ mice. We also provided genetic evidence to support that p53 functionally acts downstream of c-Abl in postnatal bone development.

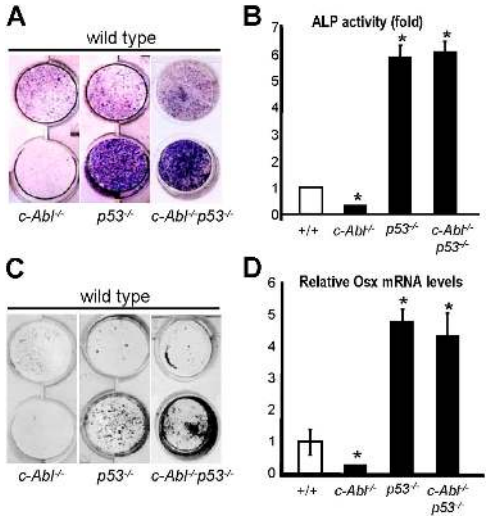


Figure 7. **Osteoblasts deficient for both p53 and c-Abl showed advanced differentiation.** Compound knockout and control osteoblasts were isolated from two litters, plated, and stained for ALP (A), quantitative ALP (B), von Kossa (C), and for assessment of osterix mRNA levels (D). The level of osterix of control osteoblasts at day 0 was set at 1. Error bars represent ± SD. Asterisks mark samples significantly different from control with $P < 0.05$.

Our findings indicate that p53 plays a role in osteoblast differentiation without directly affecting the differentiation of osteoclasts in a cell-autonomous manner. The significance of the link between p53 and bone development is underscored by the recent findings that p53 cooperates with TGF β–BMP pathways to positively regulate early development of *Xenopus laevis* (Cordenonsi et al., 2003; Takebayashi-Suzuki et al., 2003), which is in contrast to the negative role for p53 in bone homeostasis. One explanation for the opposite roles of p53 in relationship to the TGF–BMP pathways could be the timing of these two events. Mesoderm differentiation occurs at an early stage when p53 levels are high, whereas osteoblast differentiation occurs at a much later stage when p53 levels start to decline (Almog and Rotter, 1997). The inhibition of osterix by p53 may provide a mechanism to block bone development in early embryos.

Several lines of experiments suggest that p53 inhibits osteoblast differentiation as a result of repressing the expression of the lineage-specific transcription factor osterix. First, the in vivo and in vitro data indicate that osterix, but not other tested transcription factors, was elevated in the absence of p53. Second, when p53 was up-regulated, osterix expression was repressed and osteoblast differentiation was impeded. Third, BMP2-induced osterix expression was enhanced in the absence of p53. Fourth, $p53^{-/-}$ osteoblast differentiation could not be effectively repressed by c-Abl deficiency, consistent with sustained expression of osterix under this condition. Moreover, p53 was found to inhibit the promoter activity of osterix, whereas some mutant forms of p53 failed to do so. Finally, we found that the osterix levels are an important determinant in osteoblast differentiation, as the overexpression of osterix led to enhanced differentiation and the knocking down of osterix led to reduced differentiation in p53-deficient osteoblasts. Our findings might provide the first example in which p53-mediated gene repression has a physiological impact on postnatal development of the mouse. Our results suggest that p53 might do so by inhibiting osterix promoter activity by the minimal promoter independent of its binding to the upstream activation sequence. There is an increasing number of genes that are controlled by the core promoter sequence, including the TATA box (minimal promoter), and it is also becoming evident that general transcription factors, such as the thyroxine-binding protein (TBP) and TATA-binding protein-associated factors, which are associated to the core promoter sequences, can selectively regulate the transcription of certain genes (Green, 2000; Hochheimer and Tjian, 2003). Moreover, p53 also forms a complex with p300/cyclic AMP response element–binding protein, which interacts with the basal transcription machinery (Vo and Goodman, 2001). Our results suggest that p53 might repress *Osx* expression by repressing p300. Still, exactly how p53 regulates transcription of *Osx* warrants further investigation.

Our findings indicate that p53 has a cell-autonomous role in osteoblast differentiation and proliferation. It is also reported that Li-Fraumeni syndrome patients develop osteosarcoma as a component tumor and that p53 is mutated in 24 to 42% of osteosarcoma (Toguchida et al., 1992; Varley, 2003). Osteosarcoma is usually developed from osteoblasts and is related to periods in life with rapid bone growth. These observations suggest that p53 plays an important function in bone growth. More interestingly, osterix has been implicated in osteosarcoma development, as osterix is down-regulated in both human and mouse osteosarcoma cell lines and transfection of osterix into osteosarcoma cells inhibits their growth (Cao et al., 2005). It will be interesting to determine whether down-regulation of osterix is related to the p53 status in osteosarcoma cells. In many tumor cell lines, p53 is mutated but its expression is greatly up-regulated. Depending on the nature of the mutations, up-regulated p53 may repress osterix expression. For example, a hot-spot mutation, R273H, can still repress osterix promoter activity.

Osterix is an Sp1-like transcription factor that has been studied in the early development of mouse. It is essential for osteoblast maturation. Osterix has three Zinc-finger domains and is able to bind to consensus Sp1-binding sites (Nakashima et al., 2002). We show that p53 deficiency results in the elevation of osterix and enhanced osteoblastogenesis. Cell culture studies confirmed that osterix is sufficient and necessary for osteoblast differentiation. Our results also suggest that osterix regulates the expression of M-CSF to control osteoclastogenesis. M-CSF actually contains in its promoter an Sp1-binding site, which mediates the effects of estrogen on M-CSF expression and osteoclastogenesis (Srivastava et al., 1999). It is likely that osterix directly controls M-CSF expression. Recent studies revealed that transcription factors involved in osteoblast differentiation also regulate osteoclast differentiation through controlling RANKL and OPG expression. In differentiated osteoblasts, Wnt pathway and TCF1/4 were found to regulate the expression of OPG and osteoclast differentiation (Glass et al., 2005). ATF4, a cyclic AMP response element–related transcription factor that is essential for osteoblast differentiation and function, also regulates the expression of RANKL and, subsequently, osteoclast differentiation (Glass et al., 2005).

In summary, p53-deficient mice show an osteosclerotic phenotype, which is a net result of increased bone formation and increased bone resorption. p53-deficient osteoblasts exhibit accelerated proliferation, enhanced differentiation, and increased osteoclastogenic activities. Enhanced differentiation can be mediated by an elevation of osterix expression, and improved osteoclastogenesis can be mediated by increased expression of M-CSF, which is also induced by elevated osterix. These findings suggest that p53 might control bone remodeling by modulating expression of osteoblast-specific transcription factor osterix.

## Materials and methods

### Mice and cell cultures

Both $p53^{-/-}$ (The Jackson Laboratory) and $c\text{-}Abl^{-/-}$ mice were crossed to C57BL/6 six times. Primary osteoblasts were isolated from newborn pups or 20-d-old embryos, as previously described (Li et al., 2000). The cells were amplified and frozen for future use. Bone marrow stromal cultures were extracted from 3–4-mo-old mice. Both calvarial osteoblasts and stromal cells were cultured in α-MEM supplemented with 15% FCS (HyClone). For osteoblast differentiation, cells were cultured in differentiation medium (α-MEM medium containing 50 μg/ml ascorbic acid and 10 mM β–glycerol-phosphate) and were re-fed every 3 d. MEFs were isolated following a previously described standard protocol (Li et al., 2004).

**Osteoclastogenesis and bone resorption assays**
For osteoclast differentiation, the bone marrow of 3–4-mo-old mice was flushed and the monocyte fraction was isolated by centrifugation on a Ficoll plus lymphocyte separation medium gradient (ICN Biomedicals), washed, seeded at $7.5 \times 10^4$ cells/well of 96-well plates, and cultured for 7 d in differentiation medium ($\alpha$-MEM containing 10% FCS [Invitrogen], 30 ng/ml M-CSF [R&D Systems], and 50 ng/ml soluble recombinant RANKL [Sigma-Aldrich]). TRAP staining was performed using an acid phosphatase kit (Sigma-Aldrich). Osteoclast resorption function was assessed by a pit formation assay on dentine slices (OsteoSite). Monocytes were cultured for 2–3 d in the presence of 30 ng/ml M-CSF and 50 ng/ml of soluble recombinant RANKL, counted, and plated onto dentine slices that were preincubated with serum for 2 h. After 7 d, the dentine slices were sonicated in 0.5 M ammonium hydroxide, stained with either Gill's Hematoxylin or Toluidine blue for 2 min, washed with water, and photographed under a light microscope (Eclipse TE 200; Nikon). The resorbed areas were measured using a densitometry system and were normalized to the number of osteoclasts in the well. Urine levels of deoxypyridinoline cross-links were determined using commercial kits (Quidel Corporation) and were normalized to urine creatinine following the manufacturer's protocols. For coculture studies, primary calvarial osteoblasts were plated at $5 \times 10^4$ per well in 24-well plates. Upon confluency, osteoclast progenitors (BMMs; $5 \times 10^5$ per 24 wells) were then plated and the cultures were complemented with $10^{-8}$ M 1, 25 $(OH)_2$ vitamin $D_3$. Multinucleated cells appeared after 6–10 d and were counted.

**Western blot analysis**
Cells were lysed in TNEN buffer (50 mM Tris, 150 mM NaCl, 5 mM EDTA, 0.5% NP-40, and 0.1% Triton X-100) supplemented with 1 mM NaF, $Na_2VO_3$, 1 mM PMSF, and 1 $\mu$g/ml of aprotonin, leupeptin, and pepstatin. Protein concentration was determined using an assay (Bio-Rad Laboratories). Proteins were resolved by SDS-PAGE and transferred to polyvinylidene difluoride membranes (Millipore). Anti-osterix was generated by injecting rabbits with a synthesized peptide (Biogenes GMBH). Anti-p53 and -p19 antibodies were purchased from Oncogene Research Products, anti-p21 antibodies were purchased from BD Biosciences, anti-p16 and -p27 antibodies were obtained from Santa Cruz Biotechnology, Inc., and anti-actin antibodies were obtained from Sigma-Aldrich.

**Luciferase assay**
The osterix promoter (fragments ranging from 0.13 to 6.0 kb from the start of transcription) was cloned into pGL3 (luciferase basic vector; Promega). Increasing amounts of p53 expression constructs, the promoter plasmid (pGL3-Osx-Luc), and renilla plasmid (internal control) were cotransfected into C2C12 or MC3T3-E1 cells. Cells were harvested 24 h later, washed with PBS, and lysed with reporter lysis buffer (Promega). TBP, p300, and p53 are expressed under the control of cytomegalovirus promoter (in pcDNA3, pXJ, and pCMV, respectively). p53 mutants (gifts from K. Löhr and M. Dobbelstein, University of Marburg, Marburg, Germany) were described previously (Roth et al., 2000). The luciferase activities were measured following the manufacturer's procedures and were normalized against the renilla activity. All transient expressions in this assay were performed in triplicate.

**Knocking down and ectopic expression of osterix**
For siRNA knocking down experiments, the following siRNA oligomers (Dharmacon) were used: siGENOME on-target duplex 1, sense: GCCAUACGCUGACCUUUCAUU; siGENOME on-target duplex 2, sense: GGGCACAGCUCGUCUGACUUU; siGENOME on-target duplex 3, sense: CAACACACCUACUCCUUGGUU; siGENOME on-target duplex 4, sense: GCAGGCAUCUCACCAGGUCUU. The control siRNA oligomer used was a nontargeting negative siRNA control pool that was transiently transfected into primary osteoblasts following the manufacturer's procedures (Dharmacon). After 3 d, cells were harvested for ALP, osteocalcin, and Western blot analysis. To express osterix in osteoblasts, a retroviral vector was constructed with osterix ORF cloned into the pMSCVpuro vector (BioMed Diagnostics). The viruses were produced by transfecting platE cells following a standard protocol (Li et al., 2004). Osterix retroviral supernatant (different dilutions) was then used to infect primary cells, followed by 3-d selection against 5 $\mu$g/ml of puromycin before being harvested for Western blot, ALP, and RT-PCR assays. Based on the level of GFP expressed in the virus, the minimum amount of retroviral supernatant that can infect $\geq$80% of the cells was set at 100%. To express osterix at different levels, different dilutions (50, 100, 150, and 200%) of retroviral supernatant were used.

**RNA isolation, RT-PCR assay, real-time PCR, and Northern blot**
Total mRNA was isolated from osteoblasts or MEF cells growing on 60- or 100-mm dishes using TRIzol reagent (GIBCO BRL) and used for Northern blot analysis as described (Li et al., 2004). Calvaria from newborn pups or 20-d-old embryos of *p53*$^{-/-}$ and wild-type littermates were isolated and homogenized in TRIzol. The extracts were frozen at $-80$°C for 1 d and thawed for RNA extraction. Total RNA was subjected to DNase treatment (Ambion) and quantitated. 5 $\mu$g of total mRNA was reverse transcribed into complementary DNA (cDNA) using AMV (Roche) reverse transcriptase. The total reaction was used in the PCR to assay for the presence of osterix, Runx2, or actin with the following primers: osterix (197 bp): forward, 5′-TGAGGAAGAAGCCCATTCAC-3′; reverse, 5′-ACTTCTTCTCCCGGGTGTG-3′. Runx2 (113 bp): forward, 5′-TGGCAGCACGCTATTAAATC-3′; reverse, 5′-TCTGCCGCTAGAATTCAAAA-3′. β-Actin (104 bp): forward, 5′-AGATGTGGATCAGCAAGCAG-3′; reverse, 5′-GCGCAAGTTAGGTTTTGTCA-3′. PCR was performed for 30 cycles of denaturation (94°C for 30 s), annealing (57°C for 30 s), extension (72°C for 1 min), and one cycle of final extension (72°C for 10 min), which was just enough to detect the PCR products of osterix and Runx2.

The detection and quantification of target mRNA was performed with semiquantitative RT-PCR. The amplification for each mRNA was performed in the linear range for RT-PCR by optimizing the template concentration and limiting the amplification cycles to below 30 to ensure exponential amplification.

In most cases, the results were further confirmed by real-time PCR, which always gave rise to a larger difference between *p53*$^{-/-}$ and control cells than RT-PCR. cDNAs obtained from osteoblast cells and calvaria of *p53*$^{-/-}$ and wild-type mice were used in the presence of specifically designed osterix primers in a 20-$\mu$l reaction mix with TaqMan MGB probe (FAM dye-labeled). The osterix expression levels were normalized by GADPH as an internal control in real-time PCR analysis according to the manufacturer's instructions (Applied Biosystems).

**Quantitation of RT-PCR and Western blot results**
RT-PCR (negative images of gels) or Western blot results were scanned with a Molecular Dynamics scanning densitometer. The relative levels of mRNA or protein of interest were then determined by measuring the intensity of the corresponding bands. All values were averages of cell cultures isolated from at least three *p53*$^{-/-}$ mice and their control littermates and were normalized to the constitutive expression of the housekeeping genes.

**In vitro osteoblast differentiation assay**
The assays were performed as previously described (Li et al., 2000). Primary osteoblasts were plated at a high density so that the plates would become confluent overnight. This was to eliminate any possible effects of disparity in osteoblast growth rates. The relative ALP activity is defined as millimoles of *p*-nitrophenol phosphate hydrolyzed per minute per milligram of total protein (units).

**In situ hybridization**
$\alpha$-$S^{35}$-UTP–labeled single-stranded RNA probes were prepared using an RNA labeling kit (DakoCytomation) following the manufacturer's procedure with slight modifications. A 200-bp mouse osterix cDNA fragment was used to generate antisense and sense probes.

**Preparation of specimens**
All mice were labeled with 15 mg/kg of calcein subcutaneously (Sigma-Aldrich) twice in an interval of 9 d before death. The right femur of each animal was dissected free of soft tissue and used for measurement of femoral bone density by a dual energy x-ray absorptiometer. The right tibia was dissected and cut into three equal parts. The right proximal tibia and tibial shaft were fixed in 70% ethanol solution for 2 d and immersed in Villanueva Osteochrome Bone Stain (Polysciences, Inc.) for 5 d. The specimens were dehydrated by sequential changes of ascending concentrations of ethanol (70, 95, and 100%) and xylene and embedded in methyl methacrylate (Eastman Organic Chemicals). Frontal sections of the proximal tibia were cut at 5 $\mu$m using a microtome (model RM2155; Leica) and cross sections of the tibial shaft proximal to the tibiofibular junction were cut at 40 $\mu$m using a diamond wire Histo-Saw machine (Delaware Diamond Knives, Inc.). All sections were coverslipped with Eukitt (Calibrated Instruments, Inc.) for static and dynamic histomorphometric analysis.

**Bone densitometry**
Right femoral bone mineral content (BMC) and bone mineral density (BMD) were determined using a dual-energy X-ray absorptiometer (model QDR-1000W; Hologic). The machine was adapted for an ultra-high-

resolution mode with line spacing of 0.0254 cm, resolution of 0.0127 cm, and a collimator of 0.9 cm diam. The bones were placed in a Petri dish. To simulate soft tissue density surrounding the bones, tap water was poured around the bones to achieve a depth of 1 cm. Results are given for BMC and for area; area BMD is calculated as BMC/area. In addition to results for total femur, the distal and mid-region of the femur were analyzed as subregions. Coefficients of variation for these measurements in our laboratory are 0.8, 1.0, and 0.6%, respectively.

**Histomorphometric analysis**

Histomorphometric parameters of cancellous and cortical bones in the proximal tibia and tibial shaft were measured with a digitizing morphometry system, which consists of an epifluorescent microscope (model BH-2; Olympus), a color video camera, and a digitizing pad (Numonics 2206) coupled to an computer (IBM) and a morphometry program OsteoMetrics (OsteoMetrics, Inc.). Measured parameters in cortical bone included total tissue area, periosteal perimeter, marrow area, endosteal perimeter, periosteal and endosteal single- and double-labeled perimeters, interlabeled widths, and intracortical resorption area. They were then used to calculate the percentage of cortical bone area ([total tissue area − marrow area − intracortical resorption area] ÷ total tissue area × 100%), the percentage of intracortical porosis ([intracortical resorption area ÷ cortical area] × 100%), and the periosteal and endosteal bone formation rate (BFR; [double labeled perimeters + single labeled perimeters ÷ 2] × [interlabeled widths ÷ interval time ÷ periosteal perimeters]) according to the standard nomenclature.

Measured parameters of cancellous bone included total tissue area, trabecular bone area and perimeter, single- and double-labeled perimeters, and interlabeled widths. They were then used to calculate the percentage of cancellous bone volume (trabecular bone area ÷ total tissue area × 100%) and cancellous BFR ([double labeled perimeters + single labeled perimeters ÷ 2] × interlabeled widths ÷ interval time ÷ trabecular perimeters). The region of bone measured in all groups is 1–4 mm from the growth plate in the proximal tibia. All measurements and calculations were referenced to the standard nomenclature.

**Image acquisition**

Staining of cell culture plates for ALP or mineralization shown in Figs. 2, 5, and 7 was photographed using a digital camera (model Coolpix 995; Nikon). Micrographs shown in Fig. 6 were visualized on a microscope (Eclipse TE200; Nikon) with Plan Fluor objectives (4×, 0.13 NA; 10×, 0.25 NA; 20×, 0.40 NA; 40×, 0.55 NA) or a dissecting microscope (model SMZ645; Nikon), which were connected to the previously mentioned digital camera. Micrographs shown in Figs. 1 and 3 were visualized and captured as described in the previous section. The images were acquired and processed using Photoshop 6.01 (Adobe). For Western blots, Northern blots, and DNA gels, the images were acquired from films or Kodak papers with a scanner (Canoscan N1240U; Canon) and processed using Photoshop 6.01.

**Statistical analysis**

Each experiment was repeated with three or more mutant and control mice. Statistical analysis was performed using an unpaired *t* test (STATISTICA software; StatSoft, Inc.). P values were provided for all in vivo results. Significant association was defined when $P < 0.05$ compared with control.

We thank Drs. Alan Porter, Bor Luen Tang, Kanaga Sabapathy, Qiang Yu, Sharon Boast, Jing Li, and Siew Cheng Wong for helpful discussions; Hang In Ian, Deyu Cai, Wai Fook Leong, Jasmine Lau, and Christine Gao for technical support; Jie Li and Bin Qi for histology work; and Drs. Kristina Löhr, and Matthias Dobbelstein for providing mutant p53 expression constructs, retroviral constructs, and cell lines.

This work was supported by the Agency for Science, Technology, and Research of the Republic of Singapore. X. Wang, H. Kua, Y. Hu, and B. Li are adjunct members of the Department of Medicine of the National University of Singapore.

Submitted: 21 July 2005
Accepted: 22 November 2005

## References

Agoff, S.N., J. Hou, D.I. Linzer, and B. Wu. 1993. Regulation of the human hsp70 promoter by p53. *Science.* 259:84–87.

Almog, N., and V. Rotter. 1997. Involvement of p53 in cell differentiation and development. *Biochim. Biophys. Acta.* 1333:F1–F27.

Boyle, W.J., W.S. Simonet, and D.L. Lacey. 2003. Osteoclast differentiation and activation. *Nature.* 423:337–342.

Cao, Y., Z. Zhou, B. de Crombrugghe, K. Nakashima, H. Guan, X. Duan, S.F. Jia, and E.S. Kleinerman. 2005. Osterix, a transcription factor for osteoblast differentiation, mediates antitumor activity in murine osteosarcoma. *Cancer Res.* 65:1124–1128.

Chandar, N., L. Donehower, and N. Lanciloti. 2000. Reduction in p53 gene dosage diminishes differentiation capacity of osteoblasts. *Anticancer Res.* 20:2553–2559.

Choi, J., and L.A. Donehower. 1999. p53 in embryonic development: maintaining a fine balance. *Cell. Mol. Life Sci.* 55:38–47.

Cordenonsi, M., S. Dupont, S. Maretto, A. Insinga, C. Imbriano, and S. Piccolo. 2003. Links between tumor suppressors: p53 is required for TGF-beta gene responses by cooperating with Smads. *Cell.* 113:301–314.

Crighton, D., A. Woiwode, C. Zhang, N. Mandavia, J.P. Morton, L.J. Warnock, J. Milner, R.J. White, and D.L. Johnson. 2003. p53 represses RNA polymerase III transcription by targeting TBP and inhibiting promoter occupancy by TFIIIB. *EMBO J.* 22:2810–2820.

Deng, X., E.R. Hofmann, A. Villanueva, O. Hobert, P. Capodieci, D.R. Veach, X. Yin, L. Campodonico, A. Glekas, C. Cordon-Cardo, et al. 2004. *Caenorhabditis elegans* ABL-1 antagonizes p53-mediated germline apoptosis after ionizing irradiation. *Nat. Genet.* 36:906–912.

Donehower, L.A., M. Harvey, B.L. Slagle, M.J. McArthur, C.A. Montgomery Jr., J.S. Butel, and A. Bradley. 1992. Mice deficient for p53 are developmentally normal but susceptible to spontaneous tumours. *Nature.* 356:215–221.

Ducy, P., C. Desbois, B. Boyce, G. Pinero, B. Story, C. Dunstan, E. Smith, J. Bonadio, S. Goldstein, C. Gundberg, et al. 1996. Increased bone formation in osteocalcin-deficient mice. *Nature.* 382:448–452.

Ducy, P., R. Zhang, V. Geoffroy, A.L. Ridall, and G. Karsenty. 1997. Osf2/Cbfa1: a transcriptional activator of osteoblast differentiation. *Cell.* 89:747–754.

Ducy, P., M. Amling, S. Takeda, M. Priemel, A.F. Schilling, F.T. Beil, J. Shen, C. Vinson, J.M. Rueger, and G. Karsenty. 2000. Leptin inhibits bone formation through a hypothalamic relay: a central control of bone mass. *Cell.* 100:197–207.

Elefteriou, F., J.D. Ahn, S. Takeda, M. Starbuck, X. Yang, X. Liu, H. Kondo, W.G. Richards, T.W. Bannon, M. Noda, et al. 2005. Leptin regulation of bone resorption by the sympathetic nervous system and CART. *Nature.* 434:514–520.

Geoffroy, V., M. Kneissel, B. Fournier, A. Boyde, and P. Matthias. 2002. High bone resorption in adult aging transgenic mice overexpressing cbfa1/runx2 in cells of the osteoblastic lineage. *Mol. Cell. Biol.* 22:6222–6233.

Giaccia, A.J., and M.B. Kastan. 1998. The complexity of p53 modulation: emerging patterns from divergent signals. *Genes Dev.* 12:2973–2983.

Glass, D.A., P. Bialek, J.D. Ahn, M. Starbuck, M.S. Patel, H. Clevers, M.M. Taketo, F. Long, A.P. McMahon, R.A. Lang, and G. Karsenty. 2005. Canonical Wnt signaling in differentiated osteoblasts controls osteoclast differentiation. *Dev. Cell.* 8:751–764.

Green, M.R. 2000. TBP-associated factors (TAFIIs): multiple, selective transcriptional mediators in common complexes. *Trends Biochem. Sci.* 25:59–63.

Hall, P.A., and D.P. Lane. 1997. Tumor suppressors: a developing role for p53? *Curr. Biol.* 7:R144–R147.

Ho, J., and S. Benchimol. 2003. Transcriptional repression mediated by the p53 tumour suppressor. *Cell Death Differ.* 10:404–408.

Hochheimer, A., and R. Tjian. 2003. Diversified transcription initiation complexes expand promoter selectivity and tissue-specific gene expression. *Genes Dev.* 17:1309–1320.

Ko, L.J., and C. Prives. 1996. p53: puzzle and paradigm. *Genes Dev.* 10: 1054–1072.

Li, B., S. Boast, K. de los Santos, I. Schieren, M. Quiroz, S.L. Teitelbaum, M.M. Tondravi, and S.P. Goff. 2000. Mice deficient in Abl are osteoporotic and have defects in osteoblast maturation. *Nat. Genet.* 24:304–308.

Li, B., X. Wang, N. Rasheed, Y. Hu, S. Boast, T. Ishii, K. Nakayama, K.I. Nakayama, and S.P. Goff. 2004. Distinct roles of c-Abl and Atm in oxidative stress response are mediated by protein kinase C {delta}. *Genes Dev.* 18:1824–1837.

Manolagas, S.C., and R.L. Jilka. 1995. Bone marrow, cytokines, and bone remodeling. Emerging insights into the pathophysiology of osteoporosis. *N. Engl. J. Med.* 332:305–311.

Murphy, M., A. Hinman, and A.J. Levine. 1996. Wild-type p53 negatively regulates the expression of a microtubule-associated protein. *Genes Dev.* 10:2971–2980.

Murphy, M., J. Ahn, K.K. Walker, W.H. Hoffman, R.M. Evans, A.J. Levine, and D.L. George. 1999. Transcriptional repression by wild-type p53 uti-

lizes histone deacetylases, mediated by interaction with mSin3a. *Genes Dev.* 13:2490–2501.

Nakashima, K., X. Zhou, G. Kunkel, Z. Zhang, J.M. Deng, R.R. Behringer, and B. de Crombrugghe. 2002. The novel zinc finger-containing transcription factor osterix is required for osteoblast differentiation and bone formation. *Cell.* 108:17–29.

Oren, M. 1999. Regulation of the p53 tumor suppressor protein. *J. Biol. Chem.* 274:36031–36034.

Rocha, S., A.M. Martin, D.W. Meek, and N.D. Perkins. 2003. p53 represses cyclin D1 transcription through down regulation of Bcl-3 and inducing increased association of the p52 NF-kappaB subunit with histone deacetylase 1. *Mol. Cell. Biol.* 23:4713–4727.

Roth, J., P. Koch, A. Contente, and M. Dobbelstein. 2000. Tumor-derived mutations within the DNA-binding domain of p53 that phenotypically resemble the deletion of the proline-rich domain. *Oncogene.* 19:1834–1842.

Sabatakos, G., N.A. Sims, J. Chen, K. Aoki, M.B. Kelz, M. Amling, Y. Bouali, K. Mukhopadhyay, K. Ford, E.J. Nestler, and R. Baron. 2000. Overexpression of DeltaFosB transcription factor(s) increases bone formation and inhibits adipogenesis. *Nat. Med.* 6:985–990.

Sah, V.P., L.D. Attardi, G.J. Mulligan, B.O. Williams, R.T. Bronson, and T. Jacks. 1995. A subset of p53-deficient embryos exhibit exencephaly. *Nat. Genet.* 10:175–180.

Sakai, A., T. Sakata, S. Tanaka, R. Okazaki, N. Kunugita, T. Norimura, and T. Nakamura. 2002. Disruption of the p53 gene results in preserved trabecular bone mass and bone formation after mechanical unloading. *J. Bone Miner. Res.* 17:119–127.

Sarma, U., and A.M. Flanagan. 1996. Macrophage colony-stimulating factor induces substantial osteoclast generation and bone resorption in human bone marrow cultures. *Blood.* 88:2531–2540.

Schwartz, K.A., N.J. Lanciloti, M.K. Moore, A.L. Campione, and N. Chandar. 1999. p53 transactivity during in vitro osteoblast differentiation in a rat osteosarcoma cell line. *Mol. Carcinog.* 25:132–138.

Soussi, T., and G. Lozano. 2005. p53 mutation heterogeneity in cancer. *Biochem. Biophys. Res. Commun.* 331:834–842.

Srivastava, S., M.N. Weitzmann, S. Cenci, F.P. Ross, S. Adler, and R. Pacifici. 1999. Estrogen decreases TNF gene expression by blocking JNK activity and the resulting production of c-Jun and JunD. *J. Clin. Invest.* 104:503–513.

Suda, T., N. Takahashi, N. Udagawa, E. Jimi, M.T. Gillespie, and T.J. Martin. 1999. Modulation of osteoclast differentiation and function by the new members of the tumor necrosis factor receptor and ligand families. *Endocr. Rev.* 20:345–357.

Takebayashi-Suzuki, K., J. Funami, D. Tokumori, A. Saito, T. Watabe, K. Miyazono, A. Kanda, and A. Suzuki. 2003. Interplay between the tumor suppressor p53 and TGF beta signaling shapes embryonic body axes in *Xenopus*. *Development.* 130:3929–3939.

Tanaka, S., N. Takahashi, N. Udagawa, T. Tamura, T. Akatsu, E.R. Stanley, T. Kurokawa, and T. Suda. 1993. Macrophage colony-stimulating factor is indispensable for both proliferation and differentiation of osteoclast progenitors. *J. Clin. Invest.* 91:257–263.

Toguchida, J., T. Yamaguchi, B. Ritchie, R.L. Beauchamp, S.H. Dayton, G.E. Herrera, T. Yamamuro, Y. Kotoura, M.S. Sasaki, and J.B. Little. 1992. Mutation spectrum of the p53 gene in bone and soft tissue sarcomas. *Cancer Res.* 52:6194–6199.

Varley, J.M. 2003. Germline TP53 mutations and Li-Fraumeni syndrome. *Hum. Mutat.* 21:313–320.

Venot, C., M. Maratrat, C. Dureuil, E. Conseiller, L. Bracco, and L. Debussche. 1998. The requirement for the p53 proline-rich functional domain for mediation of apoptosis is correlated with specific PIG3 gene transactivation and with transcriptional repression. *EMBO J.* 17:4668–4679.

Vo, N., and R.H. Goodman. 2001. CREB-binding protein and p300 in transcriptional regulation. *J. Biol. Chem.* 276:13505–13508.

Vogelstein, B., D. Lane, and A.J. Levine. 2000. Surfing the p53 network. *Nature.* 408:307–310.

Whang, Y.E., C. Tran, C. Henderson, R.G. Syljuasen, N. Rozengurt, W.H. McBride, and C.L. Sawyers. 2000. c-Abl is required for development and optimal cell proliferation in the context of p53 deficiency. *Proc. Natl. Acad. Sci. USA.* 97:5486–5491.

Yang, X., K. Matsuda, P. Bialek, S. Jacquot, H.C. Masuoka, T. Schinke, L. Li, S. Brancorsini, P. Sassone-Corsi, T.M. Townes, et al. 2004. ATF4 is a substrate of RSK2 and an essential regulator of osteoblast biology; implication for Coffin-Lowry Syndrome. *Cell.* 117:387–398.

Yu, J., L. Zhang, P.M. Hwang, C. Rago, K.W. Kinzler, and B. Vogelstein. 1999. Identification and classification of p53-regulated genes. *Proc. Natl. Acad. Sci. USA.* 96:14517–14522.

Zhai, W., and L. Comai. 2000. Repression of RNA polymerase I transcription by the tumor suppressor p53. *Mol. Cell. Biol.* 20:5930–5938.